SAND2017-13082C

Evolution of Cement-Casing Interface in Wellbore Microannuli under Stress

Edward N. Matteo[1], Steven P. Gomez[1], Steven R. Sobolik[1], John C. Stormont[2], Thomas Dewers[1], and Mahmoud Reda Taha[2]

[1] Sandia National Laboratories, Albuquerque, New Mexico, USA
[2] University of New Mexico, Albuquerque, New Mexico, USA

MR13B-0315

1) Overview

Laboratory tests measured the compressibility and flow characteristics of wellbore microannuli. Specimens, consisting of a cement sheath cast on a steel casing with microannuli were subjected to confining pressures and casing pressures in a pressure vessel that allows simultaneous measurement of gas flow along the axis of the specimen. The flow was interpreted as the hydraulic aperture of the microannuli. We found the hydraulic aperture decreases as confining stress is increased. The larger the initial hydraulic aperture, the more it decreases as confining stress increases. The changes in measured hydraulic aperture correspond to changes of many orders of magnitude in permeability of the wellbore system, suggesting that microannulus response to stress changes may have a significant impact on estimates of wellbore leakage.

A finite element model of a wellbore system was developed that included elements representing the microannulus that incorporated the hyperbolic joint model. The thickness of the microannulus elements is equivalent to the hydraulic aperture. The calculated normal stress across the microannulus used in the numerical implementation was found to be similar to the applied confining pressure in the laboratory tests. The microannulus elements were found to reasonably reproduce laboratory behavior during loading from confining pressure increases. The calculated microannulus response to internal casing pressure changes was less stiff than measured, which may be due to hardening of the microannulus during testing.

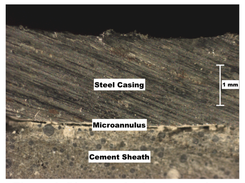

***Figure 1**. Photograph of microannulus at steel (above) and cement (below) contact.*

In particular, the microannulus model could be used to estimate CO_2 leakage as a function of formation stress changes and/or displacements, or loading from casing expansion or contraction during wellbore operations. Recommendations for future work include an application of the joint model with a thermally active large-scale reservoir coupled with pore pressure caused by dynamic CO2 injection and subsequent microannulus region affects.

2) Experimental Testing

A mock-up of a wellbore system was used for lab-scale testing. The experimental configuration is shown in Figure 2. Specimens, consisting of a cement sheath cast on a steel casing with microannuli, are subjected to confining pressures and casing pressures in a pressure vessel that allows simultaneous measurement of gas flow along the axis of the specimen. Test specimens were cast in a mold that included a central steel pipe. Class G cement was used (water/cement ratio of 0.33). The specimens were cured at 55 °C in a humid environment for a minimum of 14 days prior to testing. The finished specimens have an outer diameter of 96 mm, a casing inner diameter of 52.9 mm, and a length of 200 mm. The casing thickness varied from 1.5 to 3.2 mm between different specimens. Prior to placement in the pressure vessel, flaws were induced in the specimens. "Large microannuli" of 136 microns were created by wrapping the casing in release film prior to casting the specimen. After 24 hours, the release film and casing were removed. The casing was then reinserted into cement sheath and the specimen was allowed to cure. After curing, the casing was loose enough to slide in and out of the cement sheath (see Figure 1 above). "Small microannuli" of 19 microns were created by cooling the interior of the casing of a cured specimen with liquid nitrogen or dry ice. In response to the cooling, the casing contracted sufficiently to de-bond with the cement. Once the temperature returned to ambient, the casing remained tight in the cement sheath and there were no visible cracks or damage in the cement. In some instances, an axial force was applied to the casing to ensure it was de-bonded.

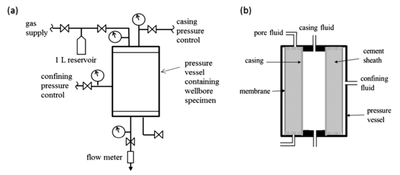

***Figure 2**. (a) Schematic of experimental configuration used to measure gas flow through cement-casing specimens under variable confining pressure and casing pressure. (b) Detail of specimen inside pressure vessel.*

The measured flowrates through the specimens with flaws were interpreted using the Forchheimer equation (Forchheimer, 1901), which includes both viscous (Darcy) and inertial (non-linear) flow terms. The Forchheimer equation can be expressed as

$$-\frac{\nabla P}{Q} = \frac{\mu}{kA} + \frac{\beta\rho}{A^2}Q \qquad (1)$$

where ∇P is the gradient, Q is the volumetric flowrate, k is the permeability, β is the inertial coefficient, A is the cross sectional area involved in the flow, μ is viscosity, and ρ is density. Plotting the left-hand side of Equation 1 vs. the flowrate yields a straight line with a slope that is a function of the inertial coefficient and an intercept proportional to permeability (Figure 3). In the absence of non-linear flow, the slope will be zero and Equation 1 reduces to Darcy's Law.

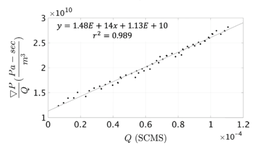

***Figure 3**. Experimental data fit to Equation 1 to decouple viscous and inertial flow components. The equation of the best linear fit to these data is used to estimate the permeability and the inertial coefficient.*

The measured The specimens featuring microannuli yielded flow rates that were more than 3 orders of magnitude greater than that for intact specimens (i.e., intact cement) under comparable conditions. Flow was therefore assumed to occur only through the flaws, and the calculated permeability was interpreted as a hydraulic aperture (h) using the so-called cubic law (Witherspoon et al., 1980)

$$h^3 = \frac{12kA}{w} \qquad (2)$$

where w is the flaw width which for these tests is the outer circumference of the casing. In the tests reported here, the flow paths were sufficiently large that gas slip effects were not observed.

3) Finite Element Modelling

Finite element models were created of the wellbore systems tested in the laboratory (see previous Section 2) in Sierra. The models include a cement sheath surrounding a steel casing; dimensions are consistent with the experimental system. The cement was modeled with the Kayenta plasticity model and the steel was assumed to behave elastically. Separate models were created to represent the interface between the cement and steel in different ways. A convergence study to determine the necessary number of elements used a full three dimensional model with a perfectly bonded interface between the steel and cement. Results from this model were compared to an analytical solution for an elastic bi-material hollow cylinder. Subsequent three-dimensional quarter-symmetric models were created using the same meshing technique, but included additional elements to explicitly represent the microannulus at the interface between the steel casing and cement sheath. The microannulus elements could be assigned as open (gap) or as a separate microannulus material. Dimensions of the two models of the laboratory wellbore configuration are illustrated by Figure 4 and Table 1. In this study the microannulus region was defined with the Kayenta constitutive model.

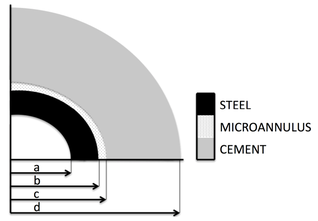

***Figure 4**. An exploded view of the laboratory wellbore model used for the parametric study. Dimensions for model utilizing this configuration are shown in Table 1 (see right).*

Table 1
Laboratory wellbore radial dimensions (mm) shown for a 2.35 mm casing with a small and large microannulus and tags referencing Fig. 4.

Location	Tag	Small microannulus (19 μm)	Large microannulus (136 μm)
Internal steel casing	a	26.475	26.475
External steel casing/internal microannulus	b	28.825	28.825
External microannulus/ internal cement sheath	c	28.844	28.961
Outer cement sheath	d	50.8	50.8

Table 2
Laboratory wellbore elastic properties used in numerical convergence simulations.

Parameter	Symbol	Unit	Value
Young's modulus: cement	E_C	Pa	4.00×10^9
Young's modulus: steel	E_S	Pa	2.00×10^{11}
Poisson's ratio: cement	ν_C	Dimensionless	0.19
Poisson's ratio: steel	ν_S	Dimensionless	0.30

Finite Stiffness elements (i.e. interfacial elements) are assigned to the microannulus regions, which are intended to capture the change in aperture of the microannulus as a function of normal stress across the microannulus using the joint stiffness model of Bandis et al (1983). These elements are shown as the region of annular joint spacing in Figure 6. Interfacial elements span the circumference between the steel casing (red) and cement sheath (yellow), where a local coordinate system (x',y',z')belonging to the Kayenta material model defines a unique orthogonal system for each interfacial block; including a normal joint direction, orientation along the joint, and direction perpendicular to both of these. These joint directions are obtained from translations on the x, y, and z coordinates, respectively. This method was used to calculate unique normal directions for joints spanning along the circumference of the microannulus region

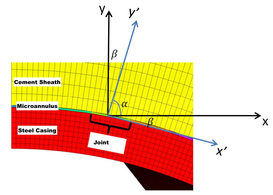

***Figure 5**. Coordinate systems used to determine stress acting across curved surface of microannulus joint.*

4) Results I – Experimental Testing

Hydraulic aperture as a function of confining pressure for a specimen with a large microannulus is shown in Figure 6. The initial hydraulic aperture was 100 microns at a confining pressure of 4 MPa. With increasing confining pressure, the hydraulic aperture decreases non-linearly with increasing rate of confinement, averaging at a rate of approximately 4 micron per MPa, until a confining pressure of 20 MPa is reached. With continued increase in confining pressure above 20 MPa, the aperture decreases only slightly. In Figure 7, hydraulic apertures as a function of confining pressure for specimens with small microannuli are shown. With increasing confining pressure, the hydraulic aperture decreases. These hydraulic apertures are about one order of magnitude smaller than that for the specimens with a large microannulus.

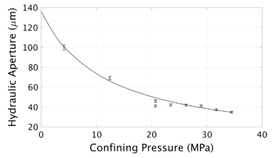

***Figure 6**. Hydraulic aperture as a function of confining pressure for specimen with large microannulus. The line is the best fit line to the hyperbolic model for these data (5% experimental error bars are shown for laboratory measured data).*

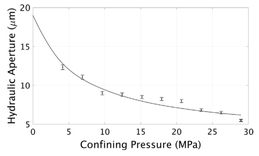

***Figure 7**. Hydraulic aperture as a function of confining pressure for specimens with small microannuli. The line is the best fit to the hyperbolic model for these data (5% experimental error bars are shown for laboratory measured data).*

The hydraulic aperture change with applied stress data given in Figures 7 and 8 are used to parameterize the hyperbolic model for a large and small microannulus. The hyperbolic model can be given in the linear form (Bandis et al., 1983)

$$\frac{\Delta V_j}{\sigma_n} = a - b\Delta V_j \qquad (3)$$

where $\frac{1}{a} = K_{ni}$, $\frac{a}{b} = V_m$ or the maximum closure, and ΔV_j is the closure of a joint under σ_n . Plotting $\frac{\Delta V}{\sigma_n}$ vs. ΔV yields a straight line with an intercept of a and a slope of –b. The hydraulic aperture data were interpreted as closure by subtracting the current aperture from the previous aperture.

5) Results II – Fitting Lab Data to Model

In Figures 8 and 9, the best fit straight line to Equation 3 is given for the experimental data measured for the large aperture and small aperture microannuli. Initial apertures (with no confining pressure) for both data sets were found by extrapolating the model response to zero normal stress; these apertures were 136 μm and 19 μm for the large and small microannuli, respectively.

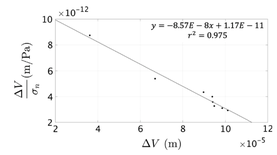

***Figure 8**. Fitting of laboratory data from small microannulus to hyperbolic model.*

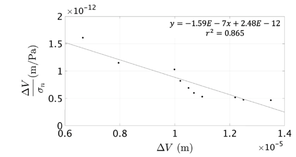

***Figure 9**. Fitting of laboratory data from small microannulus to hyperbolic model.*

Using the parameters derived from fitting the data to the hyperbolic model, the prediction for hydraulic aperture as a function of confining pressure is given in Figure 10 and 11. These results suggest that the hyperbolic model provides a reasonable representation of the measured microannulus response to confining pressure. The hyperbolic model is subsequently implemented in finite element modeling of wellbore system to describe the stress-dependent change in the hydraulic aperture and consequently permeability of a wellbore

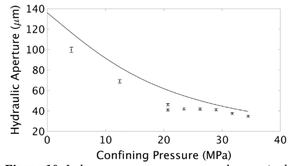

***Figure 10**. Laboratory measurements and numerical model comparison for the 136 μm microannulus joint (5% experimental error bars are shown for laboratory measured data).*

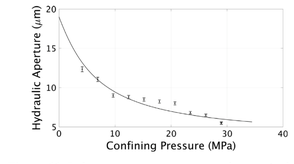

***Figure 11**. Laboratory measurements and numerical model comparison for the 19 μm microannulus joint (5% experimental error bars are shown for laboratory measured data).*

The joint parameters derived from laboratory tests were used to populate the numerical model of the microannulus. Figures 11 and 12 compare the laboratory data for the large (136 μm) and small (19 μm) microannuli with the numerical results, respectively. Both microannulus sizes were analyzed with the cement sheath parameterized with a Kayenta constitutive model. The modeled microannulus is shown to be slightly stiffer than the laboratory measured values in the 136 μm microannulus model. It is hypothesized that the occurrence of the large microannulus showing increased stiffness with respect to the small microannulus is due to furthered discontinuity between the cement and steel interface. That is, it is assumed that the microannulus is in contact throughout the circumference of the laboratory wellbore during FE computations; missing elements, voids or spaces of non-contact were not accounted for in this simulation.

6) Conclusions

We found the hydraulic aperture decreases as confining stress is increased. The larger the initial hydraulic aperture, the more it decreases as confining stress increases. The changes in measured hydraulic aperture correspond to changes of many orders of magnitude in permeability of the wellbore system, suggesting that microannulus response to stress changes may have a significant impact on estimates of wellbore leakage.

The calculated normal stress across the microannulus used in the numerical implementation was found to be similar to the applied confining pressure in the laboratory tests. The microannulus elements were found to reasonably reproduce laboratory behavior during loading from confining pressure increases. The calculated microannulus response to internal casing pressure changes was less stiff than measured, which may be due to hardening of the microannulus during testing.

References

Bandis, S.C., Lumsden, A.C., and Barton, N.R., 1983. Fundamentals of rock joint de- formation. In: International Journal of Rock Mechanics and Mining Sciences & Geomechanics Abstracts. Vol. 20. 6. Elsevier, pp. 249–268.

Forchheimer, P., 1901. Wasserbewegung durch Boden, Zeitz ver Deutch Ing., 45, 1782-1788.

Acknowledgements

Sandia National Laboratories is a multimission laboratory managed and operated by National Technology and Engineering Solutions of Sandia, LLC., a wholly owned subsidiary of Honeywell International, Inc., for the U.S. Department of Energy's National Nuclear Security Administration under contract DE-NA-0003525. SAND2017 . SAND2017-xxxx